Supporting Information

Botero et al. 10.1073/pnas.1408589111

SI Text

Modeling Environmental Predictability. Phenotypic plasticity relies on the ability to anticipate future environmental conditions. In many situations, this can be done by attending to environmental features that precede (and are correlated with) changes in relevant environmental parameters. For example, variation in day length tends to be well correlated with impending changes in temperature within temperate regions, and changes in barometric pressure often forecast approaching storms, strong winds, and heavy rain. We refer to these anticipatory events as environmental cues and model their information content by altering the degree to which they are correlated with future changes in the parameter of interest (i.e., temperature in our model). Thus, when cues are highly correlated with the parameter of interest we say that the environment is very predictable, and vice versa. We modeled environmental predictability, P, as a parameter that measures the correlation between cues, C, and environment, E, ranging from 0 (i.e., environmental cues contain no information on the potential future state of the environment) to 1 (i.e., environmental cues provide perfect information on the future state of the environment). Mathematically, environmental cues, C, are drawn in our model from a Gaussian distribution with mean

$$\mu = P \cdot E,$$

and SD

$$\sigma = (1-P)/3,$$

such that $C = E$ when $P = 1$, but C is uncorrelated with E when $P = 0$ (Fig. S1). Because 99.7% of the values in a normal distribution are contained within 3 SDs from the mean, dividing by three in the equation for sigma ensures that cues are primarily from the natural range of possible environmental values (i.e., [−1,1]). For example, at the extreme case with most variability—i.e., when $P = 0$—note that $\mu = 0$ and $3\sigma = 1$.

Genotypic Variation Within Populations. In the main text we focus on population-level responses at 50,000 generations. However, we also investigated the patterns of genotypic variation within populations, because the same kind of average outcome could be realized by either a genetically monomorphic or a genetically polymorphic population. Briefly, we observed that evolution consistently resulted in genetically monomorphic populations in our model (Fig. S2), even at the boundaries between response mode regions where average outcomes varied among replicates.

Evolutionary Transitions When Changes in Environmental Parameters Lead to Correlated Changes in the Genotype Favored by Selection. The highly consistent evolutionary outcomes observed in Fig. 2 indicate that the complex, multidimensional fitness landscape of our model tends to exhibit a single adaptive peak throughout most of parameter space. However, the evolution of different outcomes in different replicate simulations at the boundaries between response mode regions indicates that multiple adaptive peaks are likely to occur in the fitness landscape as selection shifts from favoring one outcome to another (Fig. S3).

Effects of Alternative Genotype-to-Phenotype Mapping and Algorithms for Selection. Our general findings are robust to alternative genotype-to-phenotype mapping schemes and to the consideration of evolutionary processes that may increase genetic variation within populations. Briefly, in all of the model variants that we have explored thus far, we find that a single response mode has a clear selective advantage over all others at each parameter combination and that, overall, the parameter space is divided into distinct response mode regions with relatively well-defined boundaries (Fig. S4).

To explore the effects of alternative genotype-to-phenotype mapping, we encoded norms of reaction as logistic rather than linear functions. In this model variant

$$I = 2/[1+\exp(I_0 - b \cdot C)] - 1,$$

where I_0 and b are genetically inherited traits, and C is the current value of the environmental cue.

We also evaluated the robustness of our findings to processes that may increase genetic variation within populations by exploring the effects of density- and frequency-dependent selection. Negative density-dependent selection was implemented via the standard Beverton-Holt equation for population dynamics (1), where the total number of individuals in the next generation is a function of current population size. Thus, in the density dependent variant of our model, the number of offspring for individual i was drawn from a Poisson distribution with mean, $\mu = G \cdot W_i / W_{max}$, where G is the per capita growth factor and $W_{\max}$ is the payoff an individual would accrue if it paid no costs and were able to match the exact temperature of its environment every time step of its life. The per capita growth factor, G, in this equation was computed as

$$G = \beta/(1+\alpha \cdot N),$$

where α and β are constants ($\alpha = 0.00001$ and $\beta = 2$ in Fig. S4*C*), and N is the current adult population size. To prevent unbounded population growth, excess offspring were selected at random and removed from the population whenever the new population size exceeded a carrying capacity of 5,000 individuals.

In the model variant with frequency-dependent selection, W_i was weighted by the uniqueness of an individual's phenotype. Here, a rare phenotype advantage was implemented by computing time step-specific payoffs as

$$W_{i,t} = \exp\left(-|E_t - I_{i,t}| \cdot \tau\right) \cdot \left[1 - \exp\left(-|\bar{I} - I| \cdot \varphi\right)\right],$$

where I is the mean insulation phenotype for the entire population, $I_{i,t}$ is the insulation phenotype of individual i at time step t, and ϕ is a constant that determines how strongly fitness improves for more unique individual insulation values ($\tau = 2$ and $\phi = 2$ in Fig. S4*D*). The cumulative payoff, W_i, for individual i in this model variant was then computed as the sum total of payoffs throughout its lifetime minus any costs of phenotypic adjustment. Thus

$$W_i = \sum_{t=0}^{L} W_{i,t},$$

for nonplastic individuals and

$$W_i = \sum_{t=0}^{L} W_{i,t} - k_d - n \cdot k_a,$$

for plastic individuals.

Effects of Variation in Maximal Fecundity on Extinction Rates After Environmental Change. Fig. S6 depicts the potential for extinction at each parameter combination (inner squares) as well as during transitions between adjacent combinations in parameter space for different values of q—i.e., the average number of offspring that an individual produces when it pays no plasticity costs and is able to exactly match its environment at every time step of its life. When reproductive output is low (smaller q), a major component of extinction during transition is related to the high baseline levels of extinction when moving into environments that vary quickly and are fairly unpredictable. As q increases, baseline levels of extinction are radically reduced. However, the challenges of restructuring the genome to achieve a new optimum remain whenever crossing into a new response mode region.

Interpreting Model Results in the Context of Global Climate Change. Our model investigates evolutionary responses to any type of change in the characteristics of the environment, irrespective of scale and causes. However, in this section, we provide a nontechnical overview of how our model may apply, in particular, to the highly relevant context of global environmental change. The recent past has seen an unparalleled and rapid rise in mean temperatures and sea levels around the globe, as well as a corresponding increase in the frequency and unpredictability of extreme weather events (2–5). Our model addresses these potential environmental changes in the following ways:

Rapid change in mean environmental conditions. Earth's climate exhibits multiple types of oscillations, each of which operates at different timescales. For example, in addition to the yearly changes in precipitation and temperature that define our seasons, quasi-periodic phenomena like the El Niño/Southern Oscillation can influence environmental conditions and change the intensity of climatic extremes every 2–7 y (6). Similarly, temporal variation in Earth's orbit around the sun can lead to gradual changes in mean environmental parameters on much longer timescales, ultimately resulting in phenomena like the glacial and interglacial periods (7). We have become increasingly aware in recent years that anthropogenic activity has resulted in changes to these underlying environmental cycles (2, 6). Our model allows us to explore the effects of such disturbances through changes in the parameter that controls the relative timescale of variation, R. In the main text we define R as the number of environmental oscillations per lifespan. Thus, to study the potential effects of speeding up the rate at which environmental conditions vary, we can evaluate how populations respond when transitioning into regions of parameter space with lower R. When considering the potential effects of a given environmental change, we emphasize that R is a relative index, and that as such, its value will depend on lifespan. For example, although environments that change at a rate of 1 °C/y can be approximated by a large R when considering short-lived organisms like bacteria, they are better characterized as low R when considering long-lived organisms like elephants or *Sequoia* trees. In other words, a given change in environmental cycles can potentially have very different consequences on species with different lifespans. Additionally, given that shorter lifespans increase the value of R, our model can inform us on the potential consequences of global-change-related reductions in lifespan (8) by exploring how populations respond to transitions into regions with higher R values.

Changes in the frequency and predictability of extreme weather events. It may be tempting to believe that because environmental changes are approximated in our evolutionary simulations as simple sinusoidal cycles, the world is always somewhat predictable to our virtual individuals. That, however, is not the case and therefore we emphasize again that there is an important distinction between the way that environments vary and how predictable that variation is. As demonstrated in the main text, when there is no information regarding the phase of the cycle that the environment is currently at, the manner in which environments vary is completely irrelevant to evolution [i.e., adaptive outcomes are identical whether we model environmental change as a series of stochastic events—$A = 0$, $B = 1$, and therefore, $E_t = \varepsilon$ —or as simple sinusoidal cycles—$A = 1$, $B = 0$, and therefore, $E_t = \sin(2\pi t/LR)$]. Thus, to explore the consequences of the increasing unpredictability of local environments in the context of climate change, we do not need to model increasingly irregular environmental cycles but rather alter the amount of information provided to individuals about the future states of their environment. In addition, by decoupling predictability from variability, our model provides important insights into the different effects of faster environmental change and more unpredictable conditions, both independently and in combination. Some insightful examples of how researchers have identified the use of informative environmental cues in natural systems that have evolved because of their tight correlation with future environmental conditions include work on hares (9), gulls (10), and jays (11).

1. Beverton RJH, Holt SJ (1957) *On the Dynamics of Exploited Fish Populations. Fishery Investigations Series II* (U.K. Ministry of Agriculture, Fisheries, and Food, London), Vol XIX.
2. Solomon S, et al., eds (2007) *Climate Change 2007: The Physical Science Basis* (Cambridge Univ Press, New York).
3. Bradshaw WE, Holzapfel CM (2006) Climate change. Evolutionary response to rapid climate change. *Science* 312(5779):1477–1478.
4. Norberg J, Urban MC, Vellend M, Klausmeier CA, Loeuille N (2012) Eco-evolutionary responses of biodiversity to climate change. *Nature Climate Change* 2(10):747–751.
5. Skelly DK, et al. (2007) Evolutionary responses to climate change. *Conserv Biol* 21(5): 1353–1355.
6. Meehl GA, et al. (2000) Trends in extreme weather and climate events: Issues related to modeling extremes in projections of future climate change. *Bull Am Meteorol Soc* 81(3):427–436.
7. Hays JD, Imbrie J, Shackleton NJ (1976) Variations in the Earth's orbit: Pacemaker of the Ice Ages. *Science* 194(4270):1121–1132.
8. Munch SB, Salinas S (2009) Latitudinal variation in lifespan within species is explained by the metabolic theory of ecology. *Proc Natl Acad Sci USA* 106(33):13860–13864.
9. Mills LS, et al. (2013) Camouflage mismatch in seasonal coat color due to decreased snow duration. *Proc Natl Acad Sci USA* 110(18):7360–7365.
10. Brommer JE, Rattiste K, Wilson AJ (2008) Exploring plasticity in the wild: Laying date–temperature reaction norms in the common gull *Larus canus*. *Proc R Soc B Biol Sci* 275(1635):687–693.
11. Ratikainen II, Wright J (2013) Adaptive management of body mass in Siberian jays. *Anim Behav* 85(2):427–434.

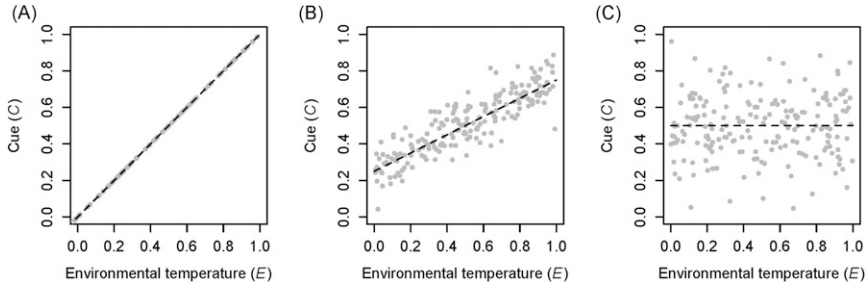

Fig. S1. Effect of predictability, *P*, on the statistical association between cues, *C*, and environmental temperatures, *E*, in our model. Plots depict cues derived from 200 randomly selected values of *E* when (*A*) $P = 1$, (*B*) $P = 0.5$, and (*C*) $P = 0$.

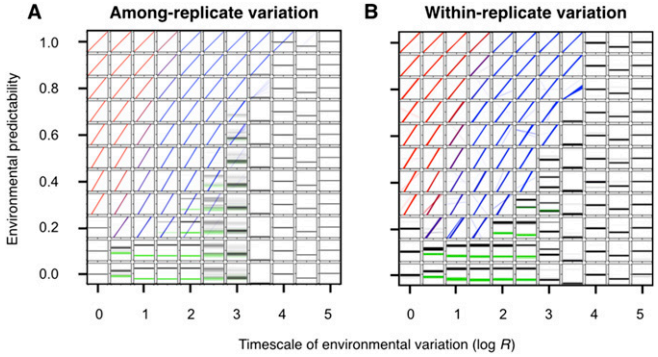

Fig. S2. Among- and within-replicate variation evolved in our model at generation 50,000. Norms of reaction are depicted as in Fig. 2, with environmental cues on the *x* axis and the resulting insulation phenotype on the *y* axis (labels omitted for simplicity). (*A*) Variation among replicates is depicted by plotting the average reaction norms for each of 100 independent replicate simulation runs (same as Fig. 2*A*). (*B*) Variation within replicates is depicted by plotting the reaction norms for each of 5,000 individuals from one representative example at each parameter combination. As in the main text, primary reaction norms are plotted in black ($s \leq 0.5$) or in a color gradient from blue ($s > 0.5$, $a = 0$) to red ($s > 0.5$, $a = 1$), and secondary reaction norms are plotted in green with more intense colors indicating that a greater number of populations or individuals share a particular response. Importantly, the coexistence of different response modes within a replicate occurs primarily at the boundaries between adjacent response mode regions.

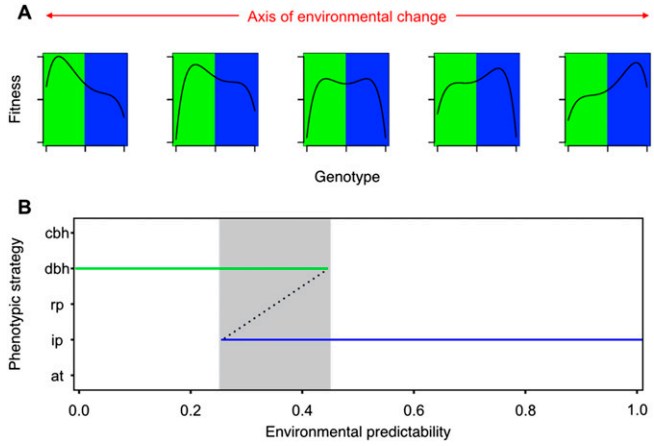

Fig. S3. Fitness landscapes illustrating the emergence of evolutionary tipping points. (*A*) Plots depicting the change of an idealized 1D fitness landscape with an environmental parameter like *R* or *P*. Genotypes corresponding to different adaptive response modes are depicted in different colors. For most values of the environmental parameter, the fitness landscape exhibits a single adaptive peak, leading to a consistent evolutionary outcome in all replicate simulations. Changes in the environmental parameter correspond to (relatively small) shifts in the location of the adaptive peak, which can relatively easily be tracked by adaptive evolution. However, when the environmental parameter approaches a value corresponding to a boundary between two response mode regions, the landscape exhibits multiple adaptive peaks (middle plot in top panel), and evolutionary outcomes can therefore vary among replicate simulations. A further change in the environmental parameter corresponds to the disappearance of the earlier fitness peak, necessitating the rapid evolution to the new fitness peak that may be separated from the earlier peak by a large distance in genotype space. The hysteresis plot in *B* depicts this situation for $R = 100$ generations per environmental cycle—i.e., $\log(R) = 2$ in Fig. 2—(cbh = conservative bet hedging; dbh = diversifying bet-hedging; ip = irreversible plasticity; rp = reversible plasticity; at = adaptive tracking). At low predictability values we observe only the evolution of diversifying bet-hedging, whereas at high values we see only the evolution of irreversible (or developmental) plasticity. However, close to the boundary between these regions (depicted here in gray) we see that replicates can result in either one of these evolutionary outcomes.

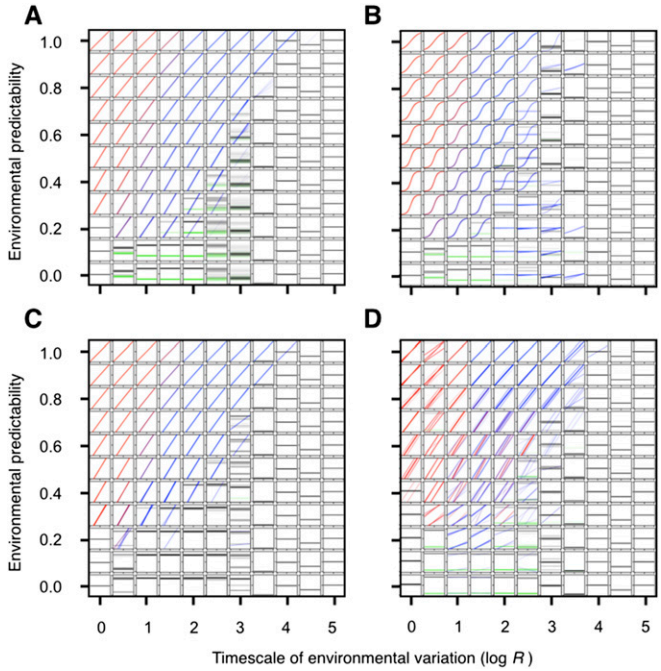

Fig. S4. Mean evolutionary outcomes at generation 50,000 for different parameter combinations under different model assumptions. (*A*) Reaction norms evolved under the baseline model described in the main text (same as depicted in Fig. 2). (*B*) Reaction norms evolved under the model variant with alternative genotype-to-phenotype mapping (i.e., reaction norms encoded as logistic rather than linear functions). (*C*) Reaction norms evolved under the model variant with negative density-dependent selection implemented through Beverton-Holt population dynamics. (*D*) Reaction norms evolved under the model variant with negative frequency-dependent selection implemented through a rare phenotype advantage. Ten replicate simulations are depicted per subplot in *B*–*D* and 100 replicates per subplot are depicted in *A*. Note that similar response mode regions are observable across the different model variants.

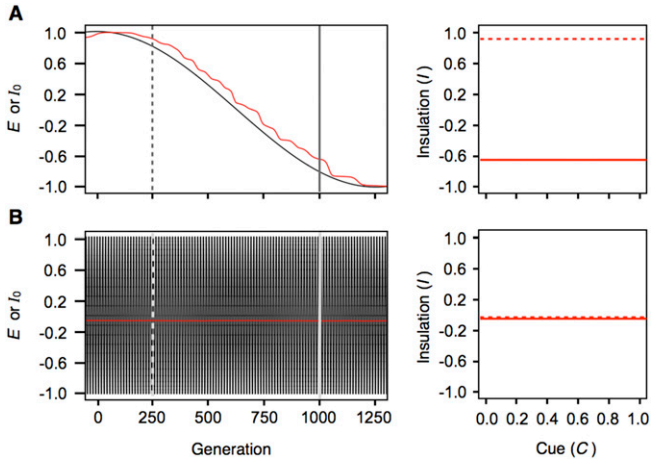

Fig. S5. Adaptive tracking vs. conservative bet-hedging in highly unpredictable environments (here $P = 0$). Environmental cycles are depicted in black and the mean population phenotypic value of I_0 is depicted in red. The evolved norms of reaction at generations 250 (dashed lines) and 1,000 (continuous lines) are shown to the right of each plot. (*A*) When environments change very slowly (here $\log R = 3$), norms of reaction evolve accordingly through mutation and natural selection, leading to phenotypic changes in the population over time. (*B*) In contrast, when environments change very rapidly (here $\log R = 0$), adaptive tracking is not possible and a phenotype that matches the average value of environmental conditions (i.e., $I_0 \sim 0$) becomes fixed.

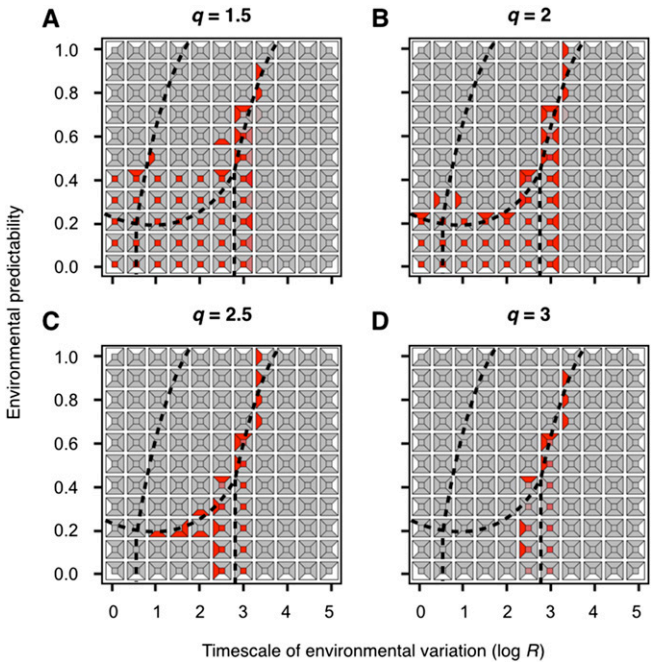

Fig. S6. Effects of reproductive potential on relative rates of extinction during transition into a new set of environmental parameters. Each subplot within each panel depicts the baseline level of extinction at a given parameter combination (inner square), and the relative extinction rates (see main text for details) associated with transitioning into the nearest parameter combination to the top, bottom, left, and right of that cell (trapezoids). Colors depict the gradient of extinction from 0% (gray) to ≥100% (red). For comparison purposes, the boundaries between response mode regions in Fig. 2*B* are presented as dashed lines. When reproductive output is low (smaller *q*; *A* and *B*), a major component of extinction during transition is related to the high baseline levels of extinction when moving into environments that vary quickly and are fairly unpredictable. As *q* increases (*C* and *D*), the baseline levels of extinction decrease considerably throughout parameter space but the challenges of restructuring the genome to achieve a new optimum remain whenever crossing into new response mode regions.

Table S1. Phenotypic implications of the main reaction norms evolved in our model

Reaction norm	Phenotypic implications
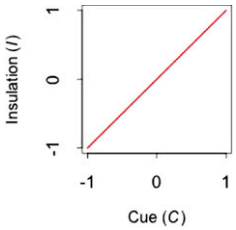	Individuals produce more insulation at higher levels of the environmental cue ($s > 0.5$ and b or $b' \sim 1$) Individuals adjust their phenotype every time step after development ($a \sim 1$) Adaptive mode: reversible plasticity
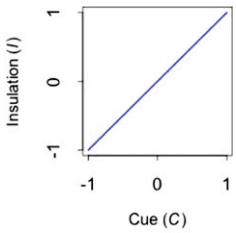	Individuals produce more insulation at higher levels of the environmental cue ($s > 0.5$ and b or $b' \sim 1$) Individuals are plastic during development but do not adjust their phenotype afterward ($a \sim 0$) Adaptive mode: irreversible plasticity
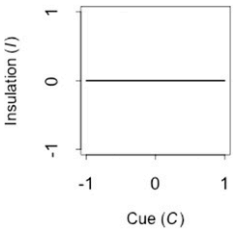	Individuals produce a single, nonadjustable phenotype at all possible environmental cues ($s \leq 0.5$) Adaptive mode: single, fixed reaction norms occur in two contexts in our model (see Fig. 3 for details) (*i*) In adaptive tracking, individual insulation levels closely match current environmental conditions, and mean population phenotypes vary gradually over time following the underlying environmental cycle (*ii*) In conservative bet-hedging insulation levels are always approximately zero; thus, although these individuals rarely ever match their current environmental conditions, they exhibit low variance in fitness by minimizing their average thermal mismatches over time
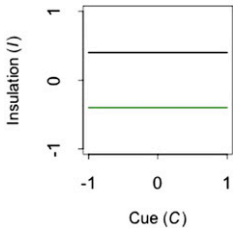	Individuals produce a single, nonadjustable phenotype at all possible environmental cues ($s \leq 0.5$) The phenotype depicted in black is produced with probability h and the one depicted in green is produced with probability $1 - h$ Adaptive mode: diversification bet-hedging